

# Heterogeneity in the *sn*-1 carbon chain of platelet-activating factor glycerophospholipids determines pro- or anti-apoptotic signaling in primary neurons<sup>S</sup>

Scott D. Ryan,<sup>\*,†</sup> Cory S. Harris,<sup>\*,†,§</sup> Casey L. Carswell,<sup>†</sup> John E. Baenziger,<sup>†</sup>  
and Steffany A. L. Bennett<sup>1,\*,†</sup>

Neural Regeneration Laboratory and Ottawa Institute of Systems Biology,<sup>\*</sup> Department of Biochemistry, Microbiology, and Immunology,<sup>†</sup> and Department of Biology,<sup>§</sup> University of Ottawa, Ottawa, Canada

**Abstract** The platelet-activating factor (PAF) family of glycerophospholipids accumulates in damaged brain tissue following injury. Little is known about the role of individual isoforms in regulating neuronal survival. Here, we compared the neurotoxic and neuroprotective activities of 1-*O*-hexadecyl-2-acetyl-*sn*-glycero-3-phosphocholine (C<sub>16</sub>-PAF) and 1-*O*-octadecyl-2-acetyl-*sn*-glycero-3-phosphocholine (C<sub>18</sub>-PAF) in cerebellar granule neurons. We find that both C<sub>16</sub>-PAF and C<sub>18</sub>-PAF cause PAF receptor-independent death but signal through different pathways. C<sub>16</sub>-PAF activates caspase-7, whereas C<sub>18</sub>-PAF triggers caspase-independent death in PAF receptor-deficient neurons. We further show that PAF receptor signaling is either pro- or anti-apoptotic, depending upon the identity of the *sn*-1 fatty acid of the PAF ligand. Activation of the PAF G-protein-coupled receptor (PAFR) by C<sub>16</sub>-PAF stimulation is anti-apoptotic and inhibits caspase-dependent death. Activation of PAFR by C<sub>18</sub>-PAF is pro-apoptotic. These results demonstrate the importance of the long-chain *sn*-1 fatty acid in regulating PAF-induced caspase-dependent apoptosis, caspase-independent neurodegeneration, and neuroprotection in the presence or absence of the PAF receptor.—Ryan, S. D., C. S. Harris, C. L. Carswell, J. E. Baenziger, and S. A. L. Bennett. Heterogeneity in the *sn*-1 carbon chain of platelet-activating factor glycerophospholipids determines pro- or anti-apoptotic signaling in primary neurons. *J. Lipid Res.* 2008. 49: 2250–2258.

**Supplementary key words** receptor • neurodegeneration • isoform • inhibitor • analog • antagonist • central nervous system • neurotoxicity • affinity • ligand

Platelet-activating factor (PAF) lipids are members of the 1-alkyl,2-acylglycerophosphocholine subclass (GP0102) of glycerophosphocholines (GP01) defined by an alkyl-ether

This work was supported by an operating grant from the Ontario Mental Health Foundation (OMHF) to S.A.L.B. S.A.L.B. is a Canadian Institutes of Health Research New Investigator and an OMHF Intermediate Investigator. S.D.R. is funded by an OMHF graduate studentship. C.S.H. is funded by a Canadian graduate studentship.

Manuscript received 19 May 2008 and in revised form 12 June 2008.

Published, JLR Papers in Press, June 12, 2008.  
DOI 10.1194/jlr.M800263-JLR200

linkage at the *sn*-1 position, an acetyl group at the *sn*-2 position, and a phosphocholine at the *sn*-3 position (1, 2) (Fig. 1). PAF species are synthesized through two enzymatic pathways (remodeling and de novo, Fig. 1). PAF-like lipids with longer *sn*-2 carbon chains or polar head group substitutions can also be produced by oxidation of structural membrane glycerophosphocholines or enzymatic modification of glycerophosphoethanolamines (Fig. 1). All three routes generate molecular species that differ in carbon chain length and degree of unsaturation at the *sn*-1 position (3). The impact of these *sn*-1 substitutions on neuronal function is not known.

The majority of PAF effects are attributed to interaction with a single G-protein-coupled receptor (PAFR). PAFR is expressed by multiple peripheral cell types but is regionally restricted to neuronal subpopulations in the central nervous system (4–6). Both PAFR-expressing and PAFR-deficient neurons are sensitive to the neurotoxic effects of PAF ligands (7, 8), yet it is not clear whether these pathways are mediated by different PAF isoforms. PAFR recognizes glycerophospholipids with an *sn*-2 acetyl moiety and an *sn*-3 phosphocholine group (1, 9). The length of the *sn*-2 carbon chain dictates PAFR affinity. Species with an *sn*-2 acetyl moiety exhibit the highest affinity (10–12). Substituting phosphoethanolamine for phosphocholine substantially reduces binding (9). The *sn*-1 ether linkage is not required for PAFR interaction but does increase potency several hundred-fold (1). The *sn*-1 carbon chain length and degree of unsaturation is implicated in activation of different PAFR signaling pathways (10, 13–15).

Abbreviations: C<sub>16</sub>-PAF, 1-*O*-hexadecyl-2-acetyl-*sn*-glycero-3-phosphocholine; C<sub>18</sub>-PAF, 1-*O*-octadecyl-2-acetyl-*sn*-glycero-3-phosphocholine; CGN, cerebellar granule neuron; CMC, critical micellar concentration; EGFP, enhanced green fluorescent protein; EMEM, Eagle's minimum essential medium; PAF, platelet-activating factor; PAFR, platelet-activating factor G-protein-coupled receptor.

<sup>1</sup>To whom correspondence should be addressed.

e-mail: sbennet@uottawa.ca

<sup>S</sup>The online version of this article (available at <http://www.jlr.org>) contains supplementary data in the form of one figure.

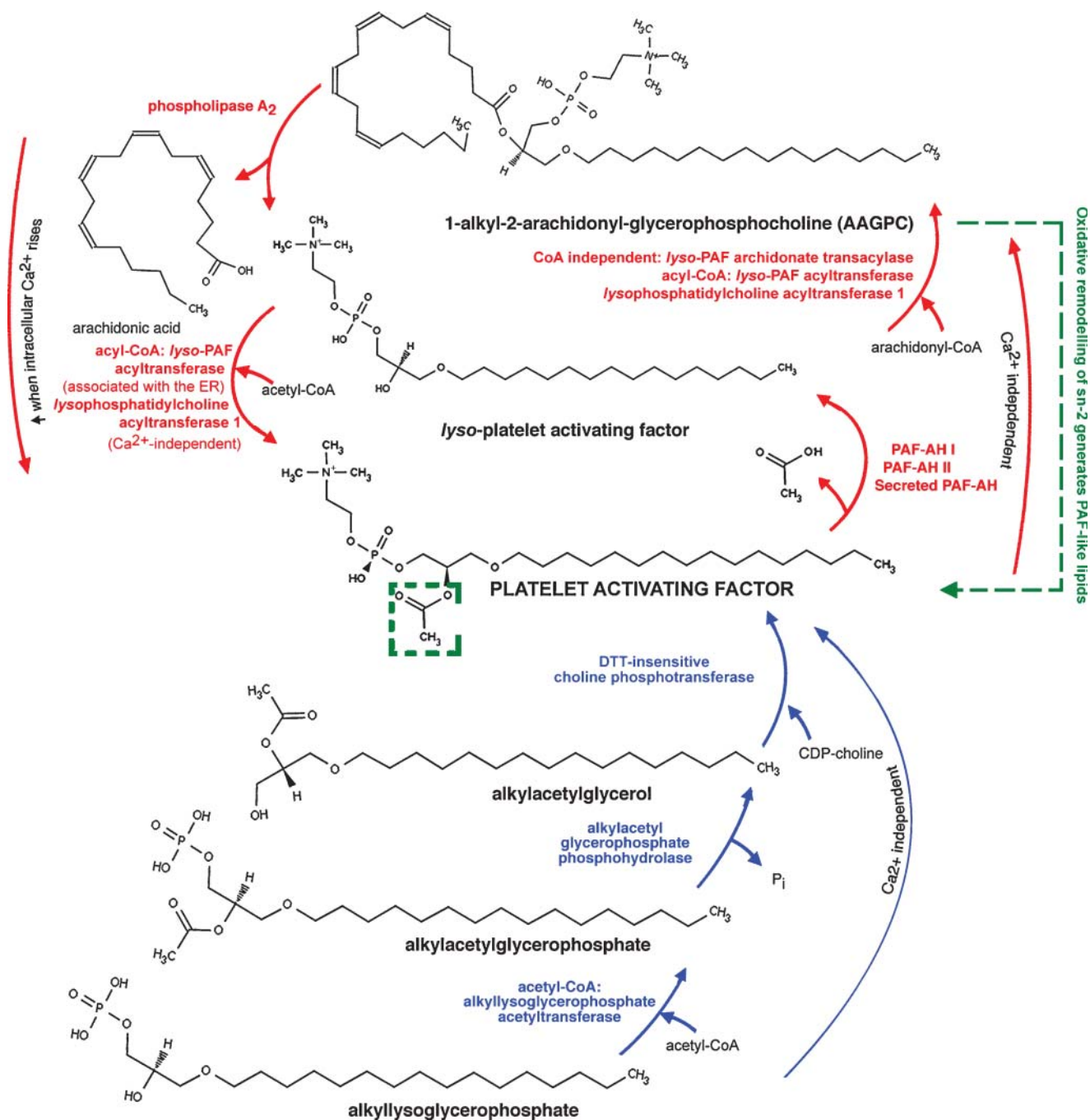


**Fig. 1.** Platelet-activating factor (PAF) metabolic pathways. PAF family members are produced through three main pathways. The primary enzymatic pathway is the remodeling pathway (red), whose kinetics in terminally differentiated neurons are faster than the de novo synthesis pathway (blue). Nonenzymatic oxidation of membrane lipids (green) generates PAF-like family members with longer-chain fatty acids (up to eight carbons) at the *sn*-2 position (hatched green box). The predominant molecular species in brain are C<sub>16</sub>-PAF and C<sub>18</sub>-PAF. Synthesis of C<sub>16</sub>-PAF from the 1-alkyl-2-arachidonyl-glycerophosphocholine parental lipid is depicted in this schematic.

These isoform-specific differences may underlie observations that PAFR expression augments chemotherapeutic cytotoxicity yet protects cells from tumor necrosis factor  $\alpha$ , TRAIL, and 1-*O*-hexadecyl-2-acetyl-*sn*-glycero-3-phosphocholine (C<sub>16</sub>-PAF) (16–19). It is not known whether different PAF isoforms initiate different pro- or anti-apoptotic signaling pathways in neurons.

Under physiological conditions, PAFs act as retrograde neurotransmitters, contributing to hippocampal CA1 long-

term potentiation by enhancing excitatory synaptic transmission (20, 21). When concentrations remain elevated, PAF lipids can initiate caspase-dependent neurotoxicity through PAFR-dependent and PAFR-independent pathways (7, 8, 22). In this regard, PAFs are recognized as primary mediators of neuronal apoptosis in acquired immune deficiency syndrome dementia, encephalitis, epileptic seizure, and ischemia (8, 22, 23). In progressive neurodegenerative disorders, PAF concentrations increase as a result of en-

hanced phospholipase A<sub>2</sub> activity (24–27). Inhibition of the PAF remodeling pathway (Fig. 1) through dietary consumption of the omega-3 polyunsaturated fatty acid docosahexaenoic acid (28) blocks PAF-mediated apoptosis in nonneural cells (29) and reduces dendritic pathology in transgenic models of Alzheimer disease (30). These changes likely involve alterations in PAF *sn*-1 isoforms. Loss of apolipoprotein E4, a risk factor associated with early-onset Alzheimer disease, alters the traffic of polyunsaturated lipids from astrocytes to neurons, skewing the composition of long-chain fatty acids in synaptosomal phosphatidylcholines from octadecyl (18:0) to hexadecyl (16:0) species (31). In relapsing-remitting multiple sclerosis, increases in plasma concentrations of 1-*O*-hexadecyl-2-acetyl-*sn*-glycero-3-phosphocholine (C<sub>16</sub>-PAF) and cerebrospinal fluid concentrations of 1-*O*-octadecyl-2-acetyl-*sn*-glycero-3-phosphocholine (C<sub>18</sub>-PAF) are associated with enhanced blood-brain barrier injury (32). The role of these different isoforms in signaling neurodegeneration is not known.

Here, we show that the carbon chain length at the *sn*-1 position dictates whether neurons undergo caspase-dependent apoptosis, caspase-independent neurodegeneration, or are protected from PAF toxicity. In PAFR-deficient neurons, we find that submicellar concentrations of C<sub>16</sub>-PAF initiate a caspase-dependent apoptotic death cascade, whereas C<sub>18</sub>-PAF signals caspase-independent degeneration. Conversely, PAFR activation by C<sub>16</sub>-PAF protects cells from PAF challenge, whereas PAFR activation by C<sub>18</sub>-PAF signals proapoptotic caspase activation. Collectively, these data implicate heterogeneity in the *sn*-1 carbon chain of PAF species in control of neuronal fate, with signaling dependent upon PAFR expression profile.

## MATERIALS AND METHODS

### Reagents

All cell culture reagents were obtained from Invitrogen (Burlington, ON) and all chemicals were purchased through Sigma-Aldrich (St. Louis, MO) unless otherwise stated. 1-*O*-hexadecyl-2-acetyl-*sn*-glycero-3-phosphocholine (C<sub>16</sub>-PAF), 1-*O*-octadecyl-2-acetyl-*sn*-glycero-3-phosphocholine (C<sub>18</sub>-PAF), and PAF antagonists were obtained from Biomol Research Laboratories (Plymouth Meeting, PA). Stock solutions of 10 mM PAF were prepared by adding vehicle (treatment media or EtOH) directly to lyophilized material in source glassware. For concentration-response studies, PAF stock and working solutions were serially diluted prior to treatment. Concentrations were verified by phosphorus assay before treatment as described in (33). In some experiments, cultures were pretreated with the PAF antagonist CV 3988 (2 μM) or antagonist vehicle (0.1% DMSO).

### Determination of critical micellar concentrations

Critical micellar concentrations (CMCs) were estimated from dynamic light-scattering data recorded on a DynaPro instrument (Wyatt Technologies, Santa Barbara, CA). For C<sub>16</sub>-PAF and C<sub>18</sub>-PAF species, 12 solutions were prepared over the concentration range of 10<sup>-7</sup> to 10<sup>-3</sup> M in 0.9 mM MgSO<sub>4</sub>, 5.4 mM KCl, 26 mM NaHCO<sub>3</sub>, 116 mM NaCl, and 1 mM NaH<sub>2</sub>PO<sub>4</sub> at pH 7.2. The mean light scattering from each solution was calculated from 10 independent measurements, each recorded at 4°C with a 10 s

acquisition time and a constant laser power. The data were analyzed using Dynamics V6 software (Wyatt Technologies). The concentration range at which micelle formation induced a dramatic increase in light scattering defined the CMC for both PAF lipid species.

### Primary murine cell culture and treatment

Breeding pairs of PAFR<sup>-/-</sup> mice (34) were kindly provided by Dr. Takao Shimizu (University of Tokyo) and Dr. Nicolas Bazan (Louisiana State University). Mice were backbred into a C57BL/6 background for 10 generations (N10), and cerebellar granule neurons (CGNs) were extracted from congenic PAFR<sup>-/-</sup> and PAFR<sup>+/+</sup> mice as previously described (7). Briefly, cerebella from postnatal day 7–10 pups were removed. The meninges were dissected, and tissue was minced in ice-cold dissection solution (124 mM NaCl, 5.37 mM KCl, 1 mM NaH<sub>2</sub>PO<sub>4</sub>, 1.2 mM MgSO<sub>4</sub>, 14.5 mM D-glucose, 25 mM Hepes, 3 mg/ml BSA, pH 7.4). Cells were dissociated in dissection media containing 0.5 mg/ml trypsin (Sigma-Aldrich) at 37°C for 18 min. Trypsin was deactivated by addition of 0.52 mg/ml chicken egg white trypsin inhibitor. Pelleted cells were resuspended in dissection solution containing 0.75 mg/ml DNase I (Roche, Mississauga, ON) and triturated to obtain a single cell suspension. CaCl<sub>2</sub> was added to a final concentration of 15 μM. CGNs were plated in Eagle's minimum essential medium (EMEM) containing 25 mM glucose, 10% FBS, 1% gentamycin, 2 mM L-glutamine, and 20 mM KCl at 37°C in a 5% CO<sub>2</sub> atmosphere at a density of 2 × 10<sup>5</sup> cells/cm<sup>2</sup> in 96-well plates coated with laminin (20 μg/ml) and poly-D-lysine (100 mg/ml). Cells were cultured in the serum-containing media for 72 h and washed extensively with PBS before being exposed to PAF in serum-free treatment media (EMEM, 25 mM glucose, 1% gentamycin, 2 mM L-glutamine, 20 mM KCl, and delipidated 0.025% BSA) as previously described (7, 35). C<sub>16</sub>-PAF and C<sub>18</sub>-PAF (0.5–1.5 μM) were dissolved in treatment media. CGNs were treated for 24 h. Where treatment with PAF antagonist CV 3988 or antagonist vehicle (0.1% DMSO) was indicated, cultures were pretreated for 15 min with test compound prior to addition of PAF isoforms. All treatments were performed in serum-free media to ensure that exogenous PAF was not hydrolyzed by serum-derived PAF acetylhydrolases. CGN survival was assessed by Live/Dead viability/cytotoxicity assay (Invitrogen). Viable cells were identified by the enzymatic conversion by intracellular esterases of nonfluorescent calcein-acetoxymethyl ester to fluorescent calcein. Dead cells were identified by uptake of ethidium homodimer as a result of loss of membrane integrity. Cells were imaged using a DMIR epifluorescent inverted microscope (Leica, Richmond Hill, ON) equipped with a QICAM digital camera (Quorum Technologies, Guelph, ON) and captured using OpenLab software v5.05 (Improvision, Lexington, MA). Percent survival was calculated as [viable cell number<sup>(calcein+ - calcein+/ET+)</sup> / mean number of viable cells in vehicle control<sup>(calcein+ - calcein+/ET+)</sup> × 100]. All procedures were carried out in agreement with the guidelines of the Canadian Council for Animal Care and as approved by the University of Ottawa Animal Care Committee.

### Recombinant adenovirus infection

Recombinant adenovirus preparation, characterization, and infection were performed as previously described (7). Briefly, recombinant adenovirus carrying enhanced green fluorescent protein (EGFP) and PAFR under separate cytomegalovirus promoters or EGFP alone was added to cell suspensions at the time of plating. All experiments were performed at a multiplicity of infection of 100 pfu/cells. Efficiency of infection of both vectors was comparable, as established by counting EGFP<sup>+</sup> cells immediately before treatment. Cell survival in serum-free media follow-

ing C<sub>16</sub>-PAF or C<sub>18</sub>-PAF (1 μM) treatment was calculated as EGFP<sup>+</sup> cell number following treatment/mean EGFP<sup>+</sup> cell number in the vehicle control × 100.

### Assessment of caspase activation

Cleavage and activation of pro-caspase 3 and pro-caspase 7 were determined by Western analysis. Proteins were isolated in RIPA buffer (10 mM PBS, 1% Nonidet P-40, 0.5% sodium deoxycholate, 0.1% SDS, 30 μl/ml aprotinin, 10 mM sodium orthovanadate, 100 μl/ml PMSF). Protein samples (30 μg) were separated by SDS-PAGE under reducing conditions. Antibodies were diluted in 1% heat-denatured casein in 10 mM PBS (10 mM sodium phosphate, 2.7 mM KCl, 4.3 mM NaCl, pH 7.5). Western analyses were performed using polyclonal anti-cleaved caspase 3 and anti-cleaved caspase 7 (1:1,000; Cell Signaling Technology, Inc., Danvers, MA) and monoclonal βIII-tubulin (1:10,000; Sigma-Aldrich, Oakville, ON). Secondary antibodies were HRP-conjugated anti-rabbit IgG (1:5,000; Jackson ImmunoResearch, Burlington, ON). Immunoreactive bands were visualized using SuperSignal West Pico (MJS BioLynx, Inc.). Caspase activation was confirmed by CaspaTag (caspase 3/7) activity assay (Chemicon, Temecula, CA) according to the manufacturer's protocol. CGNs capable of cleaving FAM-DEVD-FMK to its fluorescent product were counted and reported as a percentage of total cell number after a 24 h treatment with C<sub>16</sub>-PAF or C<sub>18</sub>-PAF (1 μM) or vehicle (treatment media). Cells were imaged as described above. Activation was confirmed by pretreatment and exposure to PAF in the presence of the caspase 3/7 inhibitor Z-DEVD-FMK (50 μM).

### Statistical analysis

Data were analyzed using one-way factorial ANOVA tests followed by post hoc Dunnett's *t*-tests. *P* values under 0.05 were considered statistically significant (shown as \*); *P* values under

0.01 or 0.001 were considered highly significant (shown as \*\* and \*\*\*, respectively).

## RESULTS

### PAFR expression protects primary CGNs from C<sub>16</sub>-PAF but not C<sub>18</sub>-PAF

PAF has been reported to elicit cell death through PAFR-dependent and PAFR-independent pathways (7, 16–18). To assess potential isoform specificity in these neurotoxic pathways, we compared the sensitivity of primary neuronal cultures endogenously expressing PAFR with cultures derived from null-mutant mice. CGNs from PAFR<sup>-/-</sup> and PAFR<sup>+/+</sup> mice were treated for 24 h with 0.5–1.5 μM C<sub>16</sub>-PAF or C<sub>18</sub>-PAF in serum-free media containing 0.025% BSA as a lipid carrier. Cell survival was assessed by Live/Dead assay. C<sub>16</sub>-PAF elicited significant concentration-dependent neuronal loss in PAFR<sup>-/-</sup> but not PAFR<sup>+/+</sup> cultures (Fig. 2A). C<sub>18</sub>-PAF initiated neuronal loss in both PAFR<sup>+/+</sup> and PAFR<sup>-/-</sup> cultures (Fig. 2B).

To confirm ligand specificity, we performed complementary gain-of-function experiments. PAFR<sup>-/-</sup> neuronal cultures were adenovirally infected with either EGFP or EGFP and human PAFR and treated with 1 μM C<sub>16</sub>-PAF or C<sub>18</sub>-PAF. C<sub>16</sub>-PAF and C<sub>18</sub>-PAF elicited neuronal death in PAFR<sup>-/-</sup> cells infected with EGFP alone (Fig. 2C, D). It should be noted that both C<sub>16</sub>- and C<sub>18</sub>-PAF (1 μM) toxicity was enhanced in cultures infected with the control virion (Fig. 2C, D), compared with uninfected cultures (Fig. 2A, B), likely due to the added stress placed on cul-

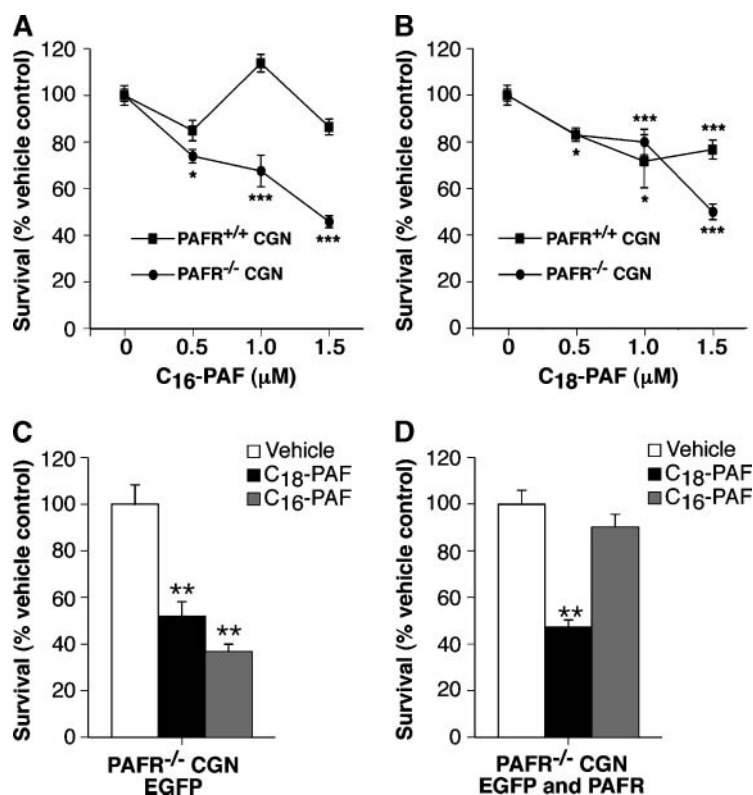


**Fig. 2.** PAF G-protein-coupled receptor (PAFR)-expressing neurons are resistant to C<sub>16</sub>-PAF but not C<sub>18</sub>-PAF toxicity. Cell survival was assessed by Live/Dead viability/cytotoxicity assay. Data are expressed as mean ± SEM. A: Both C<sub>16</sub>-PAF (0.5–1.5 μM) and C<sub>18</sub>-PAF (1–1.5 μM) were toxic to PAFR<sup>-/-</sup> cerebellar granule neurons (CGNs). B: Wild type PAFR<sup>+/+</sup> neurons were protected from C<sub>16</sub>-PAF at all concentrations tested but not C<sub>18</sub>-PAF (0.5–1.5 μM). C: Both C<sub>16</sub>-PAF (1 μM) and C<sub>18</sub>-PAF (1 μM) were toxic to PAFR<sup>-/-</sup> CGNs infected with pAdTrack-CMV adenoviral vector containing enhanced green fluorescent protein (EGFP) alone. Note that PAF-induced neuronal loss was greater in (C) compared with (A) as a result of adenoviral infection. D: Ectopic expression of PAFR using pAdTrack-CMV adenoviral vector containing EGFP and human platelet activating factor receptor-protected PAFR<sup>-/-</sup> CGNs from C<sub>16</sub>-PAF but not C<sub>18</sub>-PAF. \**P* < 0.05; \*\**P* < 0.01; \*\*\**P* < 0.001; ANOVA, post hoc Dunnett's *t*-test of PAF treatment versus vehicle treatment (n = 30–75 fields conducted in duplicate experiments).

TABLE 1. Impact of *sn*-1 chain length on critical micelle concentration of PAF species

PAF Species Member	Critical Micelle Concentration $\mu\text{M}$
C <sub>16</sub> -PAF	2.5–5.0
C <sub>18</sub> -PAF	2.5–5.0

PAF, platelet-activating factor. Critical micelle concentration (CMC) was determined on the basis of dynamic light scattering. The mean light scattering from 12 solutions of each PAF species ranging from  $10^{-7}$  to  $10^{-3}$  M was calculated from 10 independent measurements. CMC was defined as the concentration range at which a dramatic increase in light scattering was observed.

tures by the adenoviral infection itself (see supplementary Fig. 1). These data show that C<sub>16</sub>-PAF and C<sub>18</sub>-PAF elicit neuronal death in the absence of PAFR and that PAFR expression protects neurons from C<sub>16</sub>-PAF but not C<sub>18</sub>-PAF toxicity.

To address issues of nonspecific toxicity, we assessed CMC. Altering the chain length of the fatty acid present

at the *sn*-1 position of a glycerophospholipid may impact on the physicochemical properties of that molecule and thus the potential for nonspecific lytic effects. By measuring the dynamic light-scattering ability of both C<sub>16</sub>-PAF and C<sub>18</sub>-PAF at concentrations from  $10^{-3}$  to  $10^{-7}$  M, we determined that both isoforms exhibit comparable CMCs (Table 1). Because the concentrations used in assessing neurotoxicity were well below the CMCs of both lipid species, we concluded that the opposing effects of C<sub>16</sub>-PAF and C<sub>18</sub>-PAF on PAFR<sup>+/+</sup> neurons were the result of differential lipid signaling and not the result of nonspecific lytic effects.

### The identity of the PAF *sn*-1 chain dictates whether neurons undergo caspase-dependent apoptosis or caspase-independent neurodegeneration

Canonical apoptotic death is defined by caspase activation. To test whether PAF isoforms elicit neuronal apoptosis, PAFR<sup>-/-</sup> and PAFR<sup>+/+</sup> CGNs were exposed to 1  $\mu\text{M}$  C<sub>16</sub>-PAF, C<sub>18</sub>-PAF, or vehicle (treatment media). Execu-

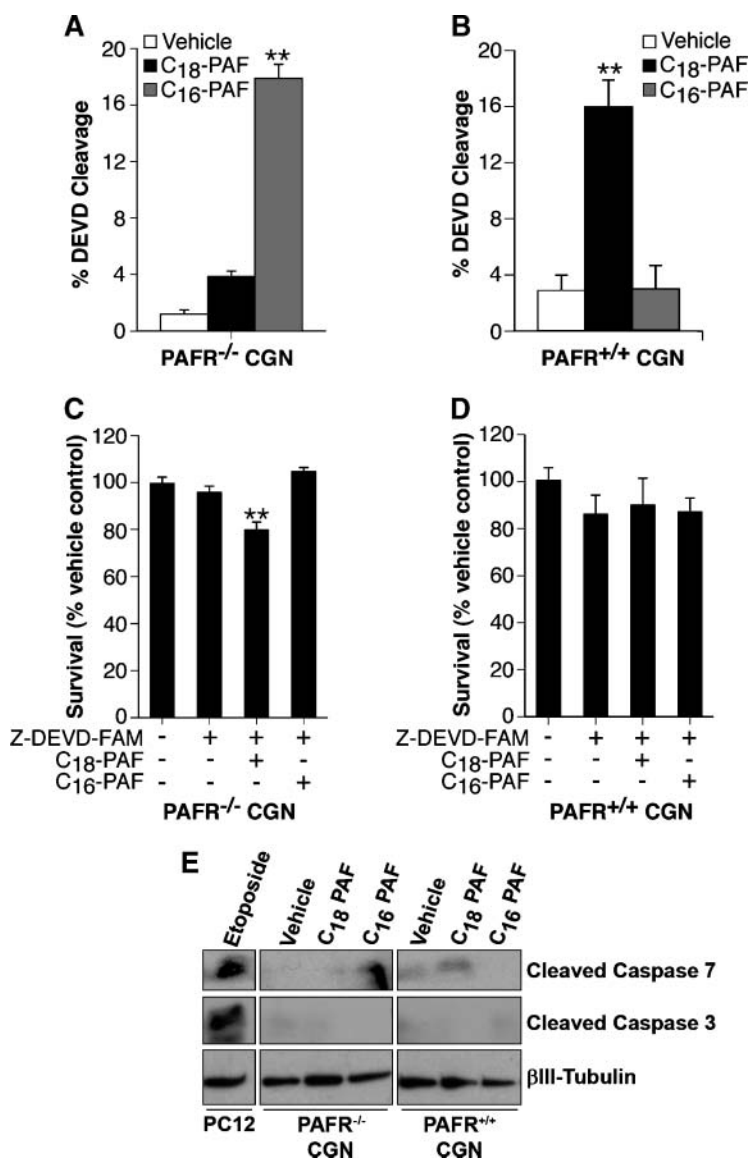


Fig. 3. PAF isoforms differentially induce caspase-dependent death in the presence or absence of PAFR. Executioner caspase 3 and 7 activation was determined using CaspaTag assay. The number of cells capable of cleaving FAM-DEVD-FMK to its fluorescent product after addition of PAF isoforms (1  $\mu\text{M}$ ) or vehicle (treatment media) was quantified after 24 h treatment. Data are expressed as the percentage of cells exhibiting DEVD cleavage (mean  $\pm$  SEM). A: PAFR<sup>-/-</sup> CGNs exhibited a significant increase in caspase 3/7 activity following C<sub>16</sub>-PAF but not C<sub>18</sub>-PAF treatment. B: C<sub>18</sub>-PAF but not C<sub>16</sub>-PAF elicited a significant increase in caspase 3/7 activity in PAFR<sup>+/+</sup> CGNs. C: Pretreatment with the irreversible caspase inhibitor Z-DEVD-FMK (50  $\mu\text{M}$ ) protected PAFR<sup>-/-</sup> CGNs from C<sub>16</sub>-PAF but not C<sub>18</sub>-PAF toxicity. D: Z-DEVD-FMK (50  $\mu\text{M}$ ) protected PAFR<sup>+/+</sup> neurons from C<sub>18</sub>-PAF toxicity. E: To confirm caspase activation, Western analysis for the active caspase 3 and caspase 7 isoforms was performed following treatment with vehicle or PAF isoform (1  $\mu\text{M}$ ). C<sub>16</sub>-PAF activated caspase 7, as indicated by cleavage of the pro-protein to its active form but not caspase 3 in PAFR<sup>-/-</sup> neurons. C<sub>18</sub>-PAF activated caspase 7 but not caspase 3 in PAFR<sup>+/+</sup> neurons. Loading control was neuron-specific  $\beta$ III-tubulin. The positive control for both caspase 3 and caspase 7 activation was etoposide-treated PC12 cells. \*\* Statistically significant ANOVA and post hoc Dunnett's *t*-test compared with vehicle with  $P < 0.01$  ( $n = 19$ –30 fields conducted in triplicate experiments).

tioner caspase 3/7 activity was determined by quantifying cleavage of the caspase 3/7 substrate FAM-DEVD-FMK (Fig. 3A, B). Despite comparable toxicity (Fig. 2A, B), C<sub>16</sub>-PAF but not C<sub>18</sub>-PAF elicited a significant increase in the number of caspase-positive PAFR<sup>-/-</sup> neurons following a 24 h treatment (Fig. 3A). By contrast, in PAFR<sup>+/+</sup> cultures, a statistically significant increase in caspase 3/7 activity was detected following C<sub>18</sub>-PAF treatment of PAFR<sup>+/+</sup> CGNs (Fig. 3B). Consistent with the observed protection conferred by PAFR expression (Fig. 2B, D), C<sub>16</sub>-PAF did not significantly activate caspase 3/7 in PAFR<sup>+/+</sup> CGNs (Fig. 3B). These data demonstrate that C<sub>16</sub>-PAF initiates caspase-dependent apoptosis in the absence of PAFR and that neurotoxicity shifts from a caspase-independent pathway to a caspase-dependent apoptotic pathway when C<sub>18</sub>-PAF activates PAFR.

To confirm that PAF isoforms differentially signal caspase-mediated apoptosis in the presence or absence of PAFR, PAFR<sup>-/-</sup> CGNs were pretreated for 15 min with the irreversible caspase 3/7 inhibitor Z-DEVD-FAM prior to PAF addition. The inhibitor was maintained in media for the duration of the PAF challenge. Preventing caspase 3/7 activation protected PAFR<sup>-/-</sup> CGNs from C<sub>16</sub>-PAF-induced apoptosis but not C<sub>18</sub>-PAF-mediated, caspase-independent death (Fig. 3C). In PAFR<sup>+/+</sup> neurons, caspase inhibition effectively blocked the C<sub>18</sub>-PAF-induced caspase-dependent apoptosis (Fig. 3D) without impacting on neuroprotection initiated by C<sub>16</sub>-PAF activation of PAFR (Fig. 3D).

Caspases 3 and 7 cleave the same consensus sequence and the same substrates (36). As such, activity assays are unable to distinguish between these caspases. However, both caspases 3 and 7 must themselves be cleaved to be activated. Using an antibody specific to cleaved caspase 7, we found that C<sub>16</sub>-PAF activated caspase 7 but not cas-

pase 3 in PAFR<sup>-/-</sup> neurons, whereas C<sub>18</sub>-PAF induced caspase 7 but not caspase 3 cleavage in PAFR<sup>+/+</sup> neurons (Fig. 3E). Taken together, these data demonstrate that C<sub>16</sub>-PAF signals the activation of executioner caspase 7 independently of PAFR, whereas C<sub>18</sub>-PAF activation of caspase 7 is PAFR dependent.

#### CV 3988 inhibits PAFR-mediated cell death activated by C<sub>18</sub>-PAF

To evaluate the effect of a competitive PAFR antagonist on these cell death pathways, PAFR<sup>-/-</sup> and PAFR<sup>+/+</sup> CGNs were exposed to PAF isoforms (1 μM) in the presence of the structural PAF analog CV 3988 (Fig. 4A, B). Control cultures were treated with antagonist vehicle (0.1% DMSO) and PAF vehicle (treatment media) for 24 h (Fig. 4A, B). Consistent with our previous results, both C<sub>16</sub>-PAF and C<sub>18</sub>-PAF were toxic to PAFR<sup>-/-</sup> CGNs (Fig. 4A, DMSO) but only C<sub>18</sub>-PAF elicited neuronal loss in PAFR<sup>+/+</sup> CGNs (Fig. 4B, DMSO). CV 3988 protected CGNs from C<sub>18</sub>-PAF-induced PAFR-dependent apoptosis (Fig. 4A, CV3988).

## DISCUSSION

In this study, we show for the first time that the length of the *sn-1* carbon chain of PAF glycerophospholipids dictates neuronal fate. We find that both C<sub>16</sub>-PAF and C<sub>18</sub>-PAF are toxic to neurons that lack PAFR but initiate different cell death pathways. When PAFR-deficient neurons are exposed to lipid ligand, C<sub>16</sub>-PAF triggers a signaling cascade culminating in the activation of executioner caspase 7, whereas C<sub>18</sub>-PAF induces caspase-independent neurodegeneration. Neurotoxicity is further modulated by PAFR expression. Ectopic or endogenous PAFR expression pro-

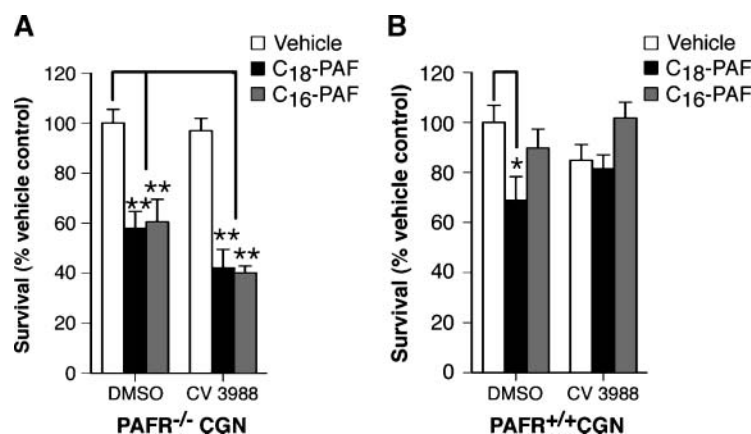


**Fig. 4.** Cell death pathways initiated by discrete PAF isoforms are inhibited by specific PAF antagonists. PAFR<sup>-/-</sup> CGNs (A) and PAFR<sup>+/+</sup> CGNs (B) were treated with C<sub>16</sub>-PAF (1 μM), C<sub>18</sub>-PAF (1 μM), or PAF vehicle (treatment media) in the presence of the competitive PAFR antagonist CV 3988 (2 μM) or antagonist vehicle (DMSO). Cell survival was assessed by Live/Dead viability/cytotoxicity assay 24 h after treatment. C<sub>16</sub>-PAF and C<sub>18</sub>-PAF were toxic to PAFR<sup>-/-</sup> neurons (A) when cultures were treated with antagonist vehicle (DMSO). Only C<sub>18</sub>-PAF was toxic to PAFR<sup>+/+</sup> neurons treated with antagonist vehicle (B, DMSO). CV 3988 protected CGNs from C<sub>18</sub>-PAF toxicity in PAFR<sup>+/+</sup> (B, CV 3988) but not PAFR<sup>-/-</sup> neurons (A, CV 3988). Data are expressed as mean ± SEM. \**P* < 0.05; \*\**P* < 0.01; ANOVA, post hoc Dunnett's *t*-test of all treatments versus PAF vehicle treated in the presence of DMSO (antagonist vehicle). (n = 25 fields conducted in duplicate experiments.)

fects neurons from C<sub>16</sub>-PAF, whereas PAFR expression shifts C<sub>18</sub>-PAF-mediated neurotoxicity from a caspase-independent to a caspase-dependent signaling pathway. These data provide insight into the underlying cell death pathways initiated following PAF challenge that, in part, reconciles reports of both pro- and anti-apoptotic PAF signaling (7, 16–18, 37, 38).

Converging evidence suggests that regional variations in the synthesis of discrete PAF isoforms are associated with neurodegenerative disease (24–28, 30–32). C<sub>16</sub>-PAF and C<sub>18</sub>-PAF are the predominant PAF species present in uninjured tissue (39, 40) but differentially accumulate over development of or following injury. Recent studies from our laboratory have shown that C<sub>16</sub>-PAF concentrations increase during neuronal differentiation (41), whereas local C<sub>18</sub>-PAF concentrations have only been shown to increase in the injured central nervous system (32). Here, we show that both C<sub>16</sub>-PAF and C<sub>18</sub>-PAF trigger neuronal death in PAFR-negative cells, but through isoform-specific apoptotic or neurodegenerative signaling pathways, respectively. Surprisingly, C<sub>16</sub>-PAF was not toxic when neurons expressed PAFR, whereas C<sub>18</sub>-PAF promoted neuronal apoptosis, shifting from caspase-independent to caspase-dependent signaling, in PAFR-competent cells. We have yet to test whether the anti-apoptotic actions of C<sub>16</sub>-PAF-PAFR are sufficient to inhibit PAF death elicited by other isoforms; however, these findings suggest that the changes in predominant *sn*-1 PAF isoforms observed over the course of neurodegenerative disease progression likely impact on the efficacy of strategies to intervene in PAF synthesis (28).

In support of such a combinatorial approach, we find that the PAFR-specific PAF analog and competitive antagonist (42) CV 3988 cannot inhibit all downstream PAF signaling pathways. CV 3988 partially rescues neurons from PAFR-dependent apoptosis resulting from C<sub>18</sub>-PAF signal transduction, consistent with its PAFR specificity; however, CV 3988 has no impact on PAF signaling in the absence of PAFR, regardless of the PAF isoform present. These data may help explain the mixed success of single PAF antagonists in therapeutic intervention (43–48). We were surprised to see that PAFR antagonism had no impact on the survival of PAFR<sup>+/+</sup> neurons treated with C<sub>16</sub>-PAF, inasmuch as we have previously reported pro-apoptotic activity in nonneuronal PC12 cells (18). Reports that CV 3988 displays inverse agonist activity may reconcile this observation (49) if inhibition of constitutive PAFR activity impacts on mitotic cell viability but not postmitotic neurons. Alternatively, C<sub>16</sub>-PAF may be more effective in competing for PAFR binding with CV 3988 than is C<sub>18</sub>-PAF.

Previous studies have attributed PAF isoform-specific bioactivity in peripheral tissue to differences in PAFR affinity (10, 13–15, 50, 51). C<sub>16</sub>-PAF has, at maximum, a 1.5- to 3-fold higher affinity for PAFR than C<sub>18</sub>-PAF, albeit with some controversy (10, 50–54). PAF stimulation of PAFR activation has been shown to elicit receptor/ligand internalization and rapid degradation of the internalized PAF to *lyso*-PAF (55–57). Thus, ligands with higher PAFR affinity (i.e., C<sub>16</sub>-PAF) are likely internalized and degraded faster than lower-affinity isoforms (i.e., C<sub>18</sub>-PAF). The net effect

would be to prevent initiation of apoptotic pathways induced by a rise in intracellular C<sub>16</sub>-PAF concentrations. In nonneuronal cells, pro- and anti-apoptotic PAF actions have been attributed to the relative ratio of NFκB-dependent pro- and anti-apoptotic gene products expressed in response to PAFR stimulation (16, 58). It may be that the lower affinity of C<sub>18</sub>-PAF for PAFR, and thus the potentially longer PAF half-life compared with C<sub>16</sub>-PAF, is sufficient to impact upon NFκB induction and that this balance shifts C<sub>18</sub>-PAF-mediated cell death from a caspase-independent to a caspase-dependent event, as has been shown in other cell systems with other pro-death ligands (59, 60).

In summary, these data illustrate that the *sn*-1 identity of PAF isoforms dictates pro- or anti-apoptotic signaling dependent upon PAFR expression status. Together, these data indicate that strategies to reduce PAF-mediated neuronal loss must take into consideration the regional expression of PAFR over the course of disease etiology as well changes in the predominant PAF isoform present in degenerating tissue. ■

The authors thank Fan Mo and Lamiaa Migahed for assistance with experiments, Jim Bennett for editorial assistance, and Dr. Shawn Whitehead for critical reading of this manuscript.

## REFERENCES

1. Prescott, S. M., G. A. Zimmerman, D. M. Stafforini, and T. M. McIntyre. 2000. Platelet activating factor and related lipid mediators. *Annu. Rev. Biochem.* **69**: 419–445.
2. LipidMaps Consortium. 2007. Lipid metabolites and pathways strategy. Accessed June 11, 2008 at <http://www.lipidmaps.org>.
3. Tokumura, A., K. Takauchi, T. Asai, K. Kamiyasu, T. Ogawa, and H. Tsukatani. 1989. Novel molecular analogues of phosphatidylcholines in a lipid extract from bovine brain: 1-long-chain acyl-2-short-chain acyl-*sn*-glycero-3-phosphocholines. *J. Lipid Res.* **30**: 219–224.
4. Mori, M., M. Aihara, K. Kume, M. Hamanoue, S. Kohsaka, and T. Shimizu. 1996. Predominant expression of platelet-activating factor receptor in rat brain microglia. *J. Neurosci.* **16**: 3590–3600.
5. Bennett, S. A. L., J. Chen, B. A. Pappas, D. C. S. Roberts, and M. Tenniswood. 1998. Platelet activating factor receptor expression is associated with neuronal apoptosis in an in vivo model of excitotoxicity. *Cell Death Differ.* **5**: 867–875.
6. Ishii, S., and T. Shimizu. 2000. Platelet-activating factor (PAF) receptor and genetically engineered PAF receptor mutant mice. *Prog. Lipid Res.* **39**: 41–82.
7. Ryan, S. D., C. S. Harris, F. Mo, H. Lee, S. T. Hou, N. G. Bazan, P. S. Haddad, J. T. Arnason, and S. A. L. Bennett. 2007. Platelet activating factor-induced neuronal apoptosis is initiated independently of its G-protein coupled PAF receptor and is inhibited by the benzoate orsellinic acid. *J. Neurochem.* **103**: 88–97.
8. Perry, S. W., J. A. Hamilton, L. W. Tjoelker, G. Dbaibo, K. A. Dzenko, L. G. Epstein, Y. Hannun, J. S. Whittaker, S. Dewhurst, and H. A. Gelbard. 1998. Platelet activating factor receptor activation. An initiator step in HIV-1 neuropathogenesis. *J. Biol. Chem.* **273**: 17660–17664.
9. O'Flaherty, J. T., T. Tessner, D. Greene, J. R. Redman, and R. L. Wykle. 1994. Comparison of 1-O-alkyl-, 1-O-alk-1'-enyl-, and 1-O-acyl-2-acetyl-*sn*-glycero-3-phosphoethanolamines and -3-phosphocholines as agonists of the platelet-activating factor family. *Biochim. Biophys. Acta.* **1210**: 209–216.
10. Carolan, E. J., and T. B. Casale. 1990. Degree of platelet activating factor-induced neutrophil migration is dependent upon the molecular species. *J. Immunol.* **145**: 2561–2565.
11. Hwang, S. B., M. H. Lam, and A. H. Hsu. 1989. Characterization of platelet-activating factor (PAF) receptor by specific binding of [<sup>3</sup>H] L-659,989, a PAF receptor antagonist, to rabbit platelet membranes:

- possible multiple conformational states of a single type of PAF receptors. *Mol. Pharmacol.* **35**: 48–58.
12. Ishii, I., T. Izumi, H. Tsukamoto, H. Umeyama, M. Ui, and T. Shimizu. 1997. Alanine exchanges of polar amino acids in the transmembrane domains of a platelet-activating factor receptor generate both constitutively active and inactive mutants. *J. Biol. Chem.* **272**: 7846–7854.
  13. Stoddart, N. R., W. E. Roudebush, and S. D. Fleming. 2001. Exogenous platelet-activating factor stimulates cell proliferation in mouse pre-implantation embryos prior to the fourth cell cycle and shows isoform-specific stimulatory effects. *Zygote*. **9**: 261–268.
  14. Handa, R. K., J. W. Strandhoy, and V. M. Buckalew, Jr. 1991. Vaso-relaxant effect of C16-PAF and C18-PAF on renal blood flow and systemic blood pressure in the anesthetized rat. *Life Sci.* **49**: 747–752.
  15. Erger, R. A., and T. B. Casale. 1996. Eosinophil migration in response to three molecular species of platelet activating factor. *Inflamm. Res.* **45**: 265–267.
  16. Li, T., M. D. Southall, Q. Yi, Y. Pei, D. Lewis, M. Al-Hassani, D. Spandau, and J. B. Travers. 2003. The epidermal platelet-activating factor receptor augments chemotherapy-induced apoptosis in human carcinoma cell lines. *J. Biol. Chem.* **278**: 16614–16621.
  17. Southall, M. D., J. S. Isenberg, H. Nakshatri, Q. Yi, Y. Pei, D. F. Spandau, and J. B. Travers. 2001. The platelet-activating factor receptor protects epidermal cells from tumor necrosis factor (TNF) alpha and TNF-related apoptosis-inducing ligand-induced apoptosis through an NF-kappa B-dependent process. *J. Biol. Chem.* **276**: 45548–45554.
  18. Brewer, C., F. Bonin, B. Bullock, M-C. Nault, J. Morin, S. Imbeault, T. Y. Shen, D. J. Franks, and S. A. L. Bennett. 2002. Platelet activating factor-induced apoptosis is inhibited by ectopic expression of the platelet activating factor G-protein coupled receptor. *J. Neurochem.* **82**: 1502–1511.
  19. Bonin, F., S. D. Ryan, L. Migahed, F. Mo, J. Lallier, D. J. Franks, H. Arai, and S. A. L. Bennett. 2004. Anti-apoptotic actions of the platelet activating factor acetylhydrolase I alpha 2 catalytic subunit. *J. Biol. Chem.* **279**: 52425–52436.
  20. Heusler, P., and G. Boehmer. 2007. Platelet-activating factor contributes to the induction of long-term potentiation in the rat somatosensory cortex in vitro. *Brain Res.* **1135**: 85–91.
  21. Chen, C., J. C. Magee, V. Marcheselli, M. Hardy, and N. G. Bazan. 2001. Attenuated LTP in hippocampal dentate gyrus neurons of mice deficient in the PAF receptor. *J. Neurophysiol.* **85**: 384–390.
  22. Bazan, N. G., B. Tu, and E. B. Rodriguez de Turco. 2002. What synaptic lipid signaling tells us about seizure-induced damage and epileptogenesis. *Prog. Brain Res.* **135**: 175–185.
  23. Birkle, D. L., P. Kurian, P. Braquet, and N. G. Bazan. 1998. Platelet activating factor antagonist BN52021 decreases accumulation of free polyunsaturated fatty acid in mouse brain during ischemia and electroconvulsive shock. *J. Neurochem.* **51**: 1900–1905.
  24. Klein, J. 2000. Membrane breakdown in acute and chronic neurodegeneration: focus on choline-containing phospholipids. *J. Neural Transm.* **107**: 1027–1063.
  25. Kanfer, J. N., G. Sorrentino, and D. S. Sitar. 1998. Phospholipases as mediators of amyloid beta peptide neurotoxicity: an early event contributing to neurodegeneration characteristic of Alzheimer's disease. *Neurosci. Lett.* **257**: 93–96.
  26. Sweet, R. A., K. Panchalingam, J. W. Pettegrew, R. J. McClure, R. L. Hamilton, O. L. Lopez, D. I. Kaufer, S. T. DeKosky, and W. E. Klunk. 2002. Psychosis in Alzheimer disease: postmortem magnetic resonance spectroscopy evidence of excess neuronal and membrane phospholipid pathology. *Neurobiol. Aging.* **23**: 547–553.
  27. Farooqui, A. A., and L. A. Horrocks. 2006. Phospholipase A2-generated lipid mediators in the brain: the good, the bad, and the ugly. *Neuroscientist.* **12**: 245–260.
  28. Watanabe, S., M. Doshi, K. Akimoto, Y. Kiso, and T. Hamazaki. 2001. Suppression of platelet-activating factor generation and modulation of arachidonate metabolism by dietary enrichment with (n-9) eicosatrienoic acid or docosahexaenoic acid in mouse peritoneal cells. *Prostaglandins Other Lipid Mediat.* **66**: 109–120.
  29. Lu, J., M. S. Caplan, D. Li, and T. Jilling. 2008. Polyunsaturated fatty acids block platelet-activating factor-induced phosphatidylinositol 3 kinase/Akt-mediated apoptosis in intestinal epithelial cells. *Am. J. Physiol. Gastrointest. Liver Physiol.* **294**: 1181–1190.
  30. Calon, F., G. P. Lim, F. Yang, T. Morhara, B. Teter, O. Ubeda, P. Rostaing, A. Triller, N. Salem, Jr., K. H. Ashe, et al. 2004. Docosahexaenoic acid protects from dendritic pathology in an Alzheimer's disease mouse model. *Neuron.* **43**: 633–645.
  31. Igbavboa, U., J. Hamilton, H. Y. Kim, G. Y. Sun, and W. G. Wood. 2002. A new role for apolipoprotein E: modulating transport of polyunsaturated phospholipid molecular species in synaptic plasma membranes. *J. Neurochem.* **80**: 255–261.
  32. Callea, L., M. Arese, A. Orlandini, C. Bargnani, A. Priori, and F. Bussolino. 1999. Platelet activating factor is elevated in cerebral spinal fluid and plasma of patients with relapsing-remitting multiple sclerosis. *J. Neuroimmunol.* **94**: 212–221.
  33. Rouser, G., A. N. Siakotos, and S. Fleischer. 1966. Quantitative analysis of phospholipids by thin-layer chromatography and phosphorus analysis of spots. *Lipids.* **1**: 85–86.
  34. Ishii, S., T. Kuwaki, T. Nagase, K. Maki, F. Tashiro, S. Sunaga, W-H. Cao, K. Kume, Y. Fukuchi, K. Ikuta, et al. 1998. Impaired anaphylactic responses with intact sensitivity to endotoxin in mice lacking a platelet activating factor receptor. *J. Exp. Med.* **187**: 1779–1788.
  35. Ammitt, A. J., and C. O'Neill. 1997. Studies of the nature of the binding by albumin of platelet-activating factor released from cells. *J. Biol. Chem.* **272**: 18772–18778.
  36. Thornberry, N. A., T. A. Rano, E. P. Peterson, D. M. Rasper, T. Timkey, M. Garcia-Calvo, V. M. Houtzager, P. A. Nordstrom, S. Roy, J. P. Vaillancourt, et al. 1997. A combinatorial approach defines specificities of members of the caspase family and granzyme B. Functional relationships established for key mediators of apoptosis. *J. Biol. Chem.* **272**: 17907–17911.
  37. Bellizzi, M. J., S. M. Lu, E. Masliah, and H. A. Gelbard. 2005. Synaptic activity becomes excitotoxic in neurons exposed to elevated levels of platelet-activating factor. *J. Clin. Invest.* **115**: 3185–3192.
  38. Zhu, P., M. A. DeCoster, and N. G. Bazan. 2004. Interplay among platelet-activating factor, oxidative stress, and group I metabotropic glutamate receptors modulates neuronal survival. *J. Neurosci. Res.* **77**: 525–531.
  39. Okumura, N., A. Fukushima, A. Igarashi, T. Sumi, T. Yamagishi, and H. Ueno. 2006. Pharmacokinetic analysis of platelet-activating factor in the tears of guinea pigs with allergic conjunctivitis. *J. Ocul. Pharmacol. Ther.* **22**: 347–352.
  40. Travers, J. B., C. Johnson, K. L. Clay, K. Harrison, T. Zekman, J. G. Morelli, and R. C. Murphy. 1997. Identification of sn-2 acetyl glycerophosphocholines in human keratinocytes. *J. Lipid Mediat. Cell Signal.* **16**: 139–145.
  41. Whitehead, S. N., W. Hou, M. Ethier, J. C. Smith, A. Bourgeois, R. Denis, S. A. L. Bennett, and D. Figeys. 2007. Rapid identification and quantitation of changes in the platelet activating factor family of glycerophospholipids over the course of neuronal differentiation by high performance liquid chromatography electrospray ionization tandem mass spectrometry. *Anal. Chem.* **79**: 8539–8548.
  42. Marcheselli, V. L., M. Rossowska, M. T. Domingo, P. Braquet, and N. G. Bazan. 1990. Distinct platelet-activating factor binding sites in synaptic endings and in intracellular membranes of rat cerebral cortex. *J. Biol. Chem.* **265**: 9140–9145.
  43. Hirashima, Y., N. Kuwayama, H. Hamada, N. Hayashi, and S. Endo. 2002. Etizolam, an anti-anxiety agent, attenuates recurrence of chronic subdural hematoma—evaluation by computed tomography. *Neurol. Med. Chir. (Tokyo).* **42**: 53–55.
  44. Brochet, B., P. Guinot, J. M. Orgogozo, C. Confavreux, L. Rumbach, and V. Laverne. 1995. Double blind placebo controlled multicentre study of ginkgolide B in treatment of acute exacerbations of multiple sclerosis. The Ginkgolide Study Group in multiple sclerosis. *J. Neurol. Neurosurg. Psychiatry.* **58**: 360–362.
  45. Akisu, M., A. Huseyinov, M. Yalaz, H. Cetin, and N. Kultursay. 2003. Selective head cooling with hypothermia suppresses the generation of platelet-activating factor in cerebrospinal fluid of newborn infants with perinatal asphyxia. *Prostaglandins Leukot. Essent. Fatty Acids.* **69**: 45–50.
  46. Hirashima, Y., S. Endo, H. Nukui, N. Kobayashi, and A. Takaku. 2001. Effect of a platelet-activating factor receptor antagonist, E5880, on cerebral vasospasm after aneurysmal subarachnoid hemorrhage—open clinical trial to investigate efficacy and safety. *Neurol. Med. Chir. (Tokyo).* **41**: 165–175.
  47. DeKosky, S. T., A. Fitzpatrick, D. G. Ives, J. Saxton, J. Williamson, O. L. Lopez, G. Burke, L. Fried, L. H. Kuller, J. Robbins, et al. 2006. The Ginkgo Evaluation of Memory (GEM) study: design and baseline data of a randomized trial of Ginkgo biloba extract in prevention of dementia. *Contemp. Clin. Trials.* **27**: 238–253.
  48. Ponto, L. L., and S. K. Schultz. 2003. Ginkgo biloba extract: review of CNS effects. *Ann. Clin. Psychiatry.* **15**: 109–119.
  49. Dupré, D. J., C. Le Gouill, M. Rola-Pleszczynski, and J. Stanková. 2001. Inverse agonist activity of selected ligands of platelet activating factor receptor. *J. Pharmacol. Exp. Ther.* **299**: 358–365.

50. Pinckard, R. N., H. J. Showell, R. Castillo, C. Lear, R. Breslow, L. M. McManus, D. S. Woodard, and J. C. Ludwig. 1992. Differential responsiveness of human neutrophils to the autocrine actions of 1-O-alkyl-homologs and 1-acyl analogs of platelet-activating factor. *J. Immunol.* **148**: 3528–3535.
51. Satouchi, K., R. N. Pinckard, and D. J. Hanahan. 1981. Influence of alkyl ether chain length of acetyl glyceryl ether phosphorylcholine and its ethanolamine analog on biological activity toward rabbit platelets. *Arch. Biochem. Biophys.* **211**: 683–688.
52. Ishii, S., T. Nagase, F. Tashiro, K. Ikuta, S. Sato, I. Waga, K. Kume, J. Miyazaki, and T. Shimizu. 1997. Bronchial hyperreactivity, increased endotoxin lethality and melanocytic tumorigenesis in transgenic mice overexpressing platelet-activating factor receptor. *EMBO J.* **16**: 133–142.
53. Shen, T. Y., S-B. Hwang, T. W. Doebber, and J. C. Robbins. 1987. The chemical and biological properties of PAF agonists, antagonists, and biosynthetic inhibitors. In *Platelet Activating Factor and Related Lipid Mediators*. F. Snyder, editor. Plenum Press, New York. 153–190.
54. Braquet, P., and J. J. Godfroid. 1987. Conformation properties of the PAF-acether receptor based on structure-activity studies. In *Platelet Activating Factor and Related Lipid Mediators*. F. Snyder, editor. Plenum Press, New York. 191–235.
55. Svetlov, S. I., K. M. Howard, M. Miwa, B. D. Flickinger, and M. S. Olson. 1996. Interaction of platelet-activating factor with rat hepatocytes: uptake, translocation, metabolism, and effects on PAF-acetylhydrolase secretion and protein tyrosine phosphorylation. *Arch. Biochem. Biophys.* **327**: 113–122.
56. Chen, J., L. Yang, J. M. Foulks, A. S. Weyrich, G. K. Marathe, and T. M. McIntyre. 2007. Intracellular PAF catabolism by PAF acetylhydrolase counteracts continual PAF synthesis. *J. Lipid Res.* **48**: 2365–2376.
57. Ohshima, N., S. Ishii, T. Izumi, and T. Shimizu. 2002. Receptor-dependent metabolism of platelet-activating factor in murine macrophages. *J. Biol. Chem.* **277**: 9722–9727.
58. Kravchenko, V. V., Z. Pan, J. Han, J. M. Herbert, R. J. Ulevitch, and R. D. Ye. 1995. Platelet-activating factor induces NF-kappaB activation through a G protein-coupled pathway. *J. Biol. Chem.* **270**: 14928–14934.
59. Okano, H., K. Shiraki, H. Inoue, Y. Yamanaka, T. Kawakita, Y. Saitou, Y. Yamaguchi, N. Enokimura, N. Yamamoto, K. Sugimoto, et al. 2003. 15-Deoxy-delta-12-14-PGJ2 regulates apoptosis induction and nuclear factor-kappaB activation via a peroxisome proliferator-activated receptor-gamma-independent mechanism in hepatocellular carcinoma. *Lab. Invest.* **83**: 1529–1539.
60. Hughes, A. L., D. Messineo-Jones, S. P. Lad, and K. E. Neet. 2001. Distinction between differentiation, cell cycle, and apoptosis signals in PC12 cells by the nerve growth factor mutant delta9/13, which is selective for the p75 neurotrophin receptor. *J. Neurosci. Res.* **63**: 10–19.